

Electron diffraction and HREM study of a short-range ordered structure in the relaxor ferroelectric $\text{Pb}(\text{Mg}_{1/3}\text{Nb}_{2/3})\text{O}_3$

Shu Miao,^{1,2} Jing Zhu,^{1,2,*} Xiaowen Zhang,^{2,3} and Z.-Y. Cheng^{1,2}

¹*Electron Microscopy Laboratory, School of Materials Science and Engineering, Tsinghua University, Beijing 100084, People's Republic of China*

²*Department of Materials Science and Engineering, Tsinghua University, Beijing 100084, People's Republic of China*

³*State Key Lab of New Ceramics and Fine Processing, Department of Materials Science and Engineering, Tsinghua University, Beijing 100084, People's Republic of China*

(Received 7 September 2001; published 27 December 2001)

A superlattice structure commonly existing in $\text{Pb}(\text{Mg}_{1/3}\text{Nb}_{2/3})\text{O}_3$ was detected by selected-area electron diffraction (SAED) and high-resolution electron microscopy (HREM). The computer simulation of the SAED and HREM showed that this superlattice structure might result from local nanosize planar antiferroelectric ordered dipoles sheets. A possible model has been proposed.

DOI: 10.1103/PhysRevB.65.052101

PACS number(s): 77.84.Dy, 61.14.Lj, 77.80.-e

Extensive investigations have been conducted on both structures and properties of $A(B'B'')\text{O}_3$ complex perovskite relaxor ferroelectrics for many years. In such a system, two different cations B' and B'' randomly occupy an equivalent lattice site. It is reasonable to deduce that the local structure is distorted and ionic shifts exist commonly due to the incompatible static electric interaction and lattice strain.

As a typical example of such materials, $\text{Pb}(\text{Mg}_{1/3}\text{Nb}_{2/3})\text{O}_3$ (PMN) attracted the most studies on its microstructure due to its technological importance as well as scientific interest.¹⁻⁴ Generally, PMN is regarded to have a simple cubic structure at room temperature.⁵⁻⁶ Data obtained by neutron-diffraction and x-ray scattering methods from bulk ceramics as well as single crystals showed an evidence of severe ionic shifts in PMN and related compounds, such as $\text{Pb}(\text{Zn}_{1/3}\text{Nb}_{2/3})\text{O}_3$ (PZN), $\text{Pb}(\text{Sc}_{1/2}\text{Nb}_{1/2})\text{O}_3$ (PSN), and $\text{Pb}(\text{Sc}_{1/2}\text{Ta}_{1/2})\text{O}_3$ (PST).⁷⁻¹⁰ Ionic displacements from ideal lattice sites may break the cubic lattice structure and lead to a local structure with lower symmetry. In addition, both electro-optic and electrostrictive effects revealed that local randomly polar microregions began to exit below T_d (the disappearing temperature of the RMS value of polarization), which is several hundred degrees above T_m (the temperature corresponding to the maximum permittivity under weak fields).^{1,11} The formation of the polar microregions requires noncubic symmetry of the crystal structure.¹ In PMN, rhombohedral symmetry structure models had been proposed on the basis of x-ray and neutron diffraction experiments.^{12,13}

The formation of random polar clusters at the room temperature was observed by Bonneau *et al.*¹⁴ and supported by a theoretical calculation of the spontaneous polarization in PMN by Gui, Gu, and Zhang.¹⁵ Recently, Gosula *et al.* studied the temperature dependence of synchrotron radiation scattering intensities from 1:1 chemical short-range order (SRO) peaks in PMN. As the temperature decreased, a change in the temperature dependence behavior was observed. They interpreted that this was due to an antiphase tilting of the oxygen octahedrons coupled with some ordering of Pb displacements at a low temperature.¹⁶

With regard to the characterization of the dielectric behavior of the relaxor ferroelectrics, various models have been proposed, such as, the superparaelectric model,¹ dipolar glass model,^{17,18} and local-electric-field model.¹⁹ Most of these models proposed the function of the randomly oriented polar microregions.

So far, all of the experiment results from neutron-diffraction and x-ray scattering methods can only disclose the average structure in bulk samples. The configuration and distribution of these polar microregions in nanosize remain unclear.

In this work, pure PMN and 5% La-doped PMN (PLMN) ceramics were studied by selected-area electron diffraction (SAED), high-resolution electron microscopy (HREM), and computer simulations. Exceptional superlattice diffraction spots at the positions $k/2\langle 110 \rangle$ and $h/3\langle 210 \rangle + m\langle 001 \rangle$ (where k , h , and m are integer numbers) with diffuse scattering were observed at the room temperature. Computer simulations of these SAED patterns, as well as HREM, were carried out based on a proposed model involving local planar antiferroelectric ordered dipoles (AFODs) sheets.

Pure PMN and PLMN powders were synthesized by using of columbite precursor as described by Swartz and ShROUT.²⁰ The ceramics were prepared by the method described in another paper²¹ in detail. Both PMN and PLMN were found to be single phase by x-ray diffraction using $\text{Cu } K\alpha$ radiation (Rigaku, Dmax-RB) generated at 40 kV and 100 mA.

Samples for transmission-electron microscopy (TEM) study were first mechanically polished to obtain a thickness of $\sim 30 \mu\text{m}$. The pellets were then thinned by ion milling (Gatan 600) until electron transparency, using a 4-kV Ar ions beam at 12° inclination. A TEM with a field emission gun operated at 200 kV (JEM-2010F, JEOL) and a double-tilt specimen holder (EM-31031, JEOL) were employed for SAED HREM. The computer simulation was performed using the EMS computer program²² and our own computer codes based on the kinematical theory.

SAED patterns of three different zone axes from a same crystal grain are shown in Figs. 1(a)–1(c). The diffraction

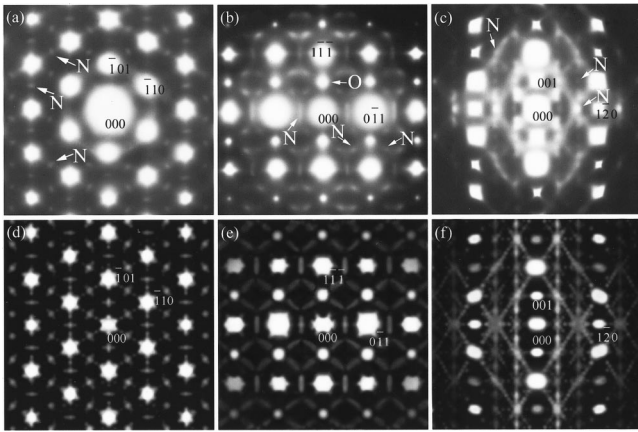


FIG. 1. Experimental and simulated SAED patterns, indexed with simple cubic indices. (a) experimental [111] zone axis; (b) experimental [211] zone axis; (c) experiment [210] zone axis; (d) simulated [111] zone axis; (e) simulated [211] zone axis; (f) simulated [210] zone axis.

spots from the disordered PMN matrix are indexed with simple cubic indices. The letter “O” denotes the $\frac{1}{2}\langle 111 \rangle$ superlattice diffraction spots from the 1:1 chemical-ordered microdomains, which were well studied by many research works.^{2,4,6} The exceptional superlattice diffraction spots are indicated by letter “N.”

Besides the superlattice spots from 1:1 chemical-ordered domains, the main features of these SAED patterns can be summarized as follows. (1) New spots at positions $k/2\langle 110 \rangle$; (2) New spots at positions $h/3\langle 210 \rangle + m\langle 001 \rangle$ with diffuse elongation along $\langle 001 \rangle$; (3) Intensities fluctuation of “N” spots along $\langle 210 \rangle$ and $\langle 001 \rangle$, respectively; and (4) Diffuse fringes along $\langle 213 \rangle$ in $\langle 210 \rangle$ zone-axis pattern. (Where k , h , and m are integer numbers.)

Because the intensities of “N” spots are very weak, long exposure time up to 30 sec was used and special contrast-balance techniques, i.e., developing the strong and the weak parts with different time, were used during films developing to show these “N” spots clearly. Therefore, strong superlattice spots from 1:1 chemical-ordered domains appeared in the same time, which are usually much weaker in conventional SAED patterns.

It is well known that the multiple scattering from strong diffracted beams can lead to extra diffraction spots in SAED patterns. The positions of spots produced through this mechanism can be predicated by simply translating the primary-diffraction pattern, so that its origin coincides successively with all the strong spots of the primary pattern.²³ The positions of the “N” spots in present study, however, cannot be obtained in this way. So these “N” spots are not obtained from multiple scattering.

Both B -site ions ordering (chemical ordering) and lattice distortion resulting from ionic shifts can produce superlattice spots in SAED patterns.^{2,24} Thus computer simulation of these SAED patterns was carried out to find the ordered structure that results in “N” spots. Kinds of chemical ordered structure models, which can give rise to $\frac{1}{3}\langle 210 \rangle$ or $\frac{1}{2}\langle 110 \rangle$, were considered to fit the patterns at beginning. But the results were unsuccessful due to the lack of the intensities

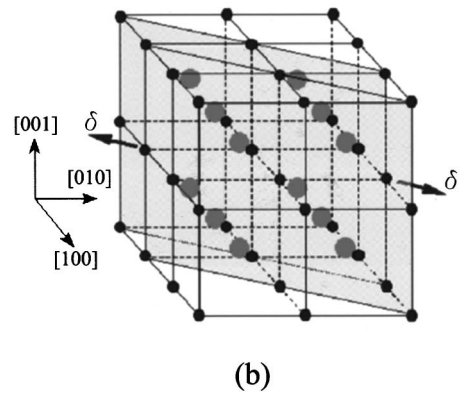
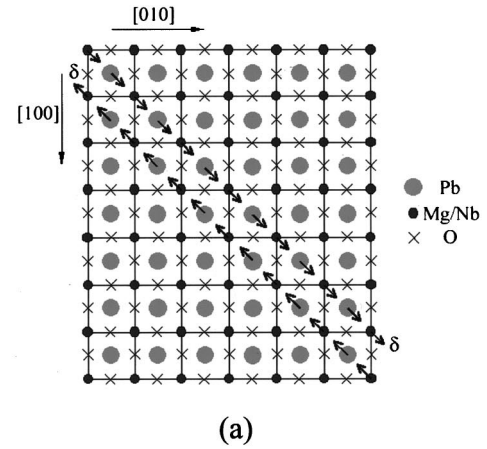


FIG. 2. Proposed planar AFODs sheet model. (a) viewed along [001] direction; (b) the three-dimensional view of the model (oxygen anions are omitted to show the model more clearly).

fluctuation of “N” spots along $\langle 210 \rangle$ and $\langle 001 \rangle$. Additionally, it is well known that La doping can greatly affect the chemical ordering of B -site ions.^{2,25} But our experiments on 5% La-doped $\text{Pb}_{0.95}\text{La}_{0.05}(\text{Mg}_{1.05/3}\text{Nb}_{1.95/3})\text{O}_3$ showed that the intensities of “N” spots remained almost the same as that from pure PMN. So it seems likely that origin of these “N” spots is structural rather than chemical.

A proposed model giving the best-matching simulated SAED patterns is shown in Figs. 2(a) and 2(b). In one unit cell of PMN, cations shift δ along [110], while in the neighboring unit cell, cations shift δ along $[\bar{1}\bar{1}0]$ ($\delta \approx 0.02$ nm). In this way an antiferroelectric dipole pair is formed. Such anti-ferroelectric dipole pairs stack along both $\langle 110 \rangle$ and $\langle 100 \rangle$, resulting in planar AFODs sheets, and produce superlattice “N” spots consequently.

Here, the displacements of oxygen ions are neglected due to the smaller atomic scattering factor of oxygen. It is difficult to estimate the exact values of the ions shift δ from SAED. By referring to other neutron-diffraction and x ray scattering data,^{7,12,26} an approximation, i.e., all cations have the same displacement about 0.02 nm in average, was made in computer simulations. This approximation will have a slight effect on the intensities of simulated “N” spots, but will not change the main features of the simulated images. In consideration of the weak intensities and diffuse nature of “N” spots, the actual coherence lengths of AFODs sheets

should be very short. In our model used for the computer simulation, coherence lengths of AFODs sheets are limited less than 5 nm. Furthermore, it was suggested by the computer simulation that these AFODs sheets are randomly distributed in PMN, orienting to every equivalent $\langle 110 \rangle$ crystallographic direction. Computer simulated patterns are shown in Figs. 1(d)–1(f). It fits the SAED patterns quite well. All the main features of Figs. 1(a)–1(c) mentioned above appear in simulated images, so this AFODs sheets model is reliable. It will be more interesting if a quantitative comparison can be made between the diffraction intensities of the experimental and the simulated patterns. However, the “N” spots are so weak that the intensity difference between the “N” spots and the primary spots overruns the dynamic ranges of the digital-recording instruments available to us, such as slow-scan charge-coupled device camera. So we cannot obtain the exact intensities of the “N” spots and primary spots simultaneously in present experiments.

Severe compositional fluctuation of *B* cations and lattice distortion were found to widely exist in PMN,²⁷ this may promote the formation of AFODs sheets. Figure 3(a) is the HREM of PMN along $[001]$ zone axis. By the fast Fourier transform (FFT), the lattice distortion of (010) and (100) planes, which contain Pb^{2+} , is clearly revealed in Fig. 3(b). In some areas, the distortions proceed along $[110]$ and $[\bar{1}\bar{1}0]$ directions. These areas may serve as an additional evidence for the existence of the planar AFODs, because this kind of distortion can be easily formed via antiphase shift of ions of neighboring unit cells. The computer-simulated FFT image, based on the model proposed above, is shown in Fig. 3(d).

Recently, Gosula *et al.* reported a change in temperature-dependence behavior of PMN and attributed it to the presence of antiferroelectric fluctuations. The discovered “N” spots and the computer simulations based on the AFODs sheets model imply that the local antiferroelectric ordering occurs even above the room temperature. This discovery of

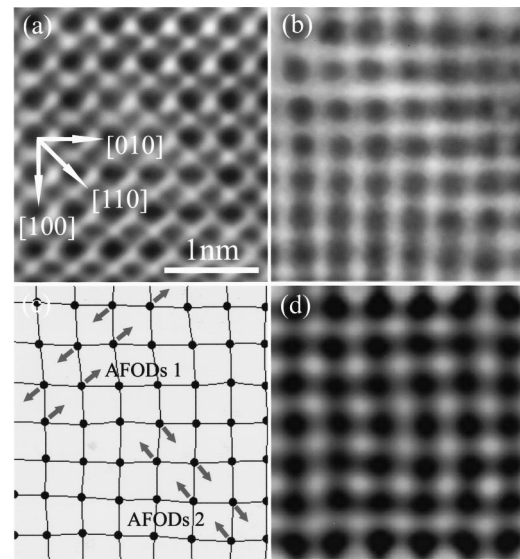


FIG. 3. (a) HREM of PMN along $[001]$ direction, Scherzer defocus = 61 nm; (b) the FFT image of (a), the (100), (010), $(\bar{1}00)$, $(0\bar{1}0)$ and transmitted reflections are used; (c) a schematic diagram of the Pb^{2+} displacements in (b); (d) the computer simulated image of (b).

the existence of nanosize AFODs sheets offers direct evidence for the concept of polar microregions. The antiferroelectric ordering may be a crucial interaction competing with ferroelectric ordering. It is possible that the competition between these two ordered states directly lead to the diffuse phase transition (DPT) and frequency dispersion in PMN.

This work was supported by the Chinese National Natural Science Foundation and National 973 project, and was partially supported by the State Key Lab of New Ceramics and Fine Processes.

*Corresponding author. FAX: 86-10-62772507; Email address: izhu@mail.tsinghua.edu.cn

¹L. E. Cross, *Ferroelectrics* **76**, 241 (1987); **151**, 305 (1994).

²J. Chen, H. M. Chan, and M. P. Harmer, *J. Am. Ceram. Soc.* **72**, 593 (1989).

³X. W. Zhang, Q. Wang, and B. L. Gu, *J. Am. Ceram. Soc.* **74**, 2846 (1991).

⁴P. K. Davies and M. A. Akbas, *J. Phys. Chem. Solids* **61**, 159 (2000).

⁵G. A. Smolenskii and A. I. Agranovskaya, *Sov. Phys. Tech. Phys.* **3**, 1380 (1958).

⁶E. Husson, M. Chubb, and A. Morell, *Mater. Res. Bull.* **23**, 357 (1988).

⁷T. Egami, W. Dmowski, S. Teslic, P. K. Davies, I.-W. Chen, and H. Chen, *Ferroelectrics* **206–207**, 231 (1998).

⁸D. M. Fanning, I. K. Robinson, X. Lu, and D. A. Payne, *J. Phys. Chem. Solids* **61**, 209 (2000).

⁹N. Takesue, Y. Fujii, M. Ichihara, and H. Chen, *Phys. Lett. B* **257**, 195 (1999).

¹⁰W. Dmowski, M. K. Akbas, P. K. Davies, and T. Egami, *J. Phys.*

Chem. Solids **61**, 229 (2000).

¹¹G. Burns and F. H. Dacol, *Solid State Commun.* **48**, 853 (1983).

¹²N. W. Thomas, S. A. Ivanov, S. Ananta, R. Tellgren, and H. Rundlof, *J. Eur. Ceram. Soc.* **19**, 2667 (1999).

¹³N. de Mathan, E. Husson, G. Calvarin, J. R. Gavarri, A. W. Hewat, and A. Morell, *J. Phys.: Condens. Matter* **3**, 8159 (1991).

¹⁴P. Bonneau, P. Garnier, G. Calvarin, E. Husson, J. R. Gavarri, A. W. Hewat, and A. Morell, *J. Solid State Chem.* **91**, 350 (1991).

¹⁵H. Gui, B.-L. Gu, and X.-W. Zhang, *Ferroelectrics* **163**, 69 (1995).

¹⁶V. Gosula, A. Tkachuk, K. Chung, and H. Chen, *J. Phys. Chem. Solids* **61**, 221 (2000).

¹⁷D. Viehland, J. Li, S. Jang, and L. E. Cross, *Phys. Rev. B* **43**, 8316 (1991).

¹⁸D. Viehland, M. Wuttig, and L. E. Cross, *Ferroelectrics* **120**, 71 (1991).

¹⁹W. Kleemann, *Int. J. Mod. Phys. B* **7**, 2469 (1993).

²⁰S. L. Swartz and T. R. Shrout, *Mater. Res. Bull.* **17**, 1245 (1982).

²¹H.-Z. Jin, Jing Zhu, Shu Miao, X. W. Zhang, and Z. Y. Cheng,

- Ceram. Trans. **118**, 191 (2000).
- ²²P. A. Stadelmann, *Ultramicroscopy* **21**, 131 (1987).
- ²³P. Hirsch, A. Howie, R. B. Nicholson, D. W. Pashley, and M. J. Whelan, *Electron Microscopy of Thin Crystals* (Robert E. Krieger, Huntington, 1977).
- ²⁴A. M. Glazer, *Acta Crystallogr., Sect. B: Struct. Crystallogr. Cryst. Chem.* **28**, 3384 (1972).
- ²⁵P. K. Davies and M. A. Akbas, *Ferroelectrics* **221**, 27 (1999).
- ²⁶M. D. Glinchuk, I. P. Bykov, and V. V. Laguta, *Ferroelectrics* **143**, 39 (1993).
- ²⁷H.-Z. Jin, Jing Zhu, Shu Miao, X. W. Zhang, and Z. Y. Cheng, *J. Appl. Phys.* **89**, 5048 (2001).